Mechanical Systems and Signal Processing (1998) **12**(5), 627–639
Article No. pg980166

STRUCTURAL MODAL TESTING WITH VARIOUS ACTUATORS AND SENSORS

B.-T. WANG

Department of Mechanical Engineering, National Pingtung University of Science and Technology, Pingtung, Taiwan 91207, Republic of China

(Received June 1997, accepted after revisions May 1998)

This paper presents the theoretical formulation of generic frequency response functions (FRFs) for continuous systems associated with various forms of actuation and sensing methods. The generic actuator and sensor eigenfunctions are identified and interpreted physically. The FRF can then be expressed in a conventional modal format. The testing procedure by roving the sensor with the fixed actuator results in the sensor eigenfunction after the extraction of modal parameters. In contrast, roving the actuator with the fixed sensor results in the actuator eigenfunction. The physical meanings of the extracted mode shapes are shown to be characterised by the form of the actuators and sensors. The lateral vibration of a one-dimensional beam problem is illustrated to demonstrate the applications of various forms of actuators and sensors to structural modal testing. Three types of actuators and three types of sensors are considered, and the feasibility of structural testing for applying any combination of the actuators and sensors is shown. This work provides the theoretical base for applying various forms of actuators and sensors to structural modal testing.

1. INTRODUCTION

Experimental modal analysis (EMA) has become a widely accepted tool for characterising the dynamic behaviour of mechanical structures. System identification, condition monitoring, trouble shooting, design optimisation, response prediction and force determination can be based on EMA techniques [1]. Conventional approaches for EMA may apply point forces such as impact hammers or shakers as actuation forces and use accelerometers as sensing devices [2–4]. Through the measurement and signal processing of input and output data, the frequency response function (FRF) can be determined. By applying curve-fitting algorithms to manipulate frequency response data, modal parameters can be estimated, and therefore the mathematical model based on a discrete multiple degree of freedom (mdof) spatial model can be derived [5].

Various excitation forms and sensing techniques are now being developed for EMA. The scanning laser Doppler vibrometer is used for structural modal testing to obtain the mode shapes successfully [6, 7]. A rotational sensing device is also available to measure rotational response [8]. Point moment excitation device is also attracting a great deal of interest. Recently, distributed piezoceramic transducers such as PZT and PVDF have received much attention in structural vibration and acoustic control [9–13]. Such distributed types of actuators and sensors have been applied to structural modal testing [14–17] instead of discrete ones. However, a complete derivation of modal testing theory for other forms of actuation and sensing methods rather than point actuation and point measurement is not yet available.

0888–3270/98/050627 + 13 $30.00/0

This paper develops a general formulation of FRFs for continuous system subject to various forms of actuation and sensing methods considering proportional damping. The generic actuator and sensor eigenfunctions (or mode shapes) depending on the forms of actuators and sensors are identified. The FRFs associated with the generic actuator and sensor eigenfunctions for continuous systems are derived and shown similar to those for a discrete mdof model. Therefore, the modal parameters extraction methods [5] for a discrete mdof system can be applied to obtain the modal model as well as the physical model.

A one-dimensional beam problem is shown to demonstrate the derivation of generic FRFs. Three types of actuation forces, point force, point moment and PZT pure bending excitation [10,11], are considered, while three types of sensing devices, accelerometer, rotational sensor [8] and PVDF sensor [12], serve as output measurement sensors. The associated actuator and sensor eigenfunctions (mode shapes) are first identified and physically interpreted. The generic FRFs associated with those actuators and sensors can then be derived. Conventional curve-fitting algorithms are applicable to extract the modal parameters. The test procedure is also noted in order to obtain a proper set of modal parameters. This work provides the theoretical base for applying various forms of actuators and sensors to structural modal testing of continuous systems.

2. THEORETICAL ANALYSIS

The partial differential equation describing the motion of a continuous system over domain D can be expressed as follows [18]:

$$L[w(P, t)] + \frac{\partial}{\partial t} C[w(P, t)] + M(P) \frac{\partial^2 w(P, t)}{\partial t^2} = f(P, t) \tag{1}$$

where L and C are linear homogeneous self-adjoint differential operators consisting of derivatives through order $2p$ with respect to the spatial coordinates P but not with respect to time t, containing the information concerning the stiffness and damping functions. $M(P)$ is the mass distribution function of the system. $f(P, t)$ is the general force function. For simplicity, the boundary conditions are assumed homogeneous so that at every point on the boundaries of domain D boundary conditions must be satisfied

$$B_i[w(P, t)] = 0, \quad i = 1, 2, \ldots, p \tag{2}$$

where B_i is the linear homogeneous differential operator containing derivatives normal to the boundary and along the boundary of order through $2p - 1$.

2.1. EIGENPROBLEM ANALYSIS

With the use of normal modes analysis, the eigenvalue problem associated with the homogeneous undamped system can be shown to be

$$L[w] = \lambda M w = \omega^2 M w. \tag{3}$$

The above equation must be satisfied over domain D, and w is subject to the boundary conditions as shown in equation (2). The eigenvalue problem is solvable. An infinite set of natural frequencies ω_r and their corresponding eigenfunctions $w_r(P)$ can then be obtained. If the eigenfunctions are orthonormal, then

$$\int_D M(P) w_r(P) w_s(P) \, \mathrm{d}D(P) = \delta_{rs} \tag{4}$$

$$\int_D w_r(P)L[w_s(P)]\,\mathrm{d}D(P) = \omega_r^2\delta_{rs} \tag{5}$$

where δ_{rs} is the Kronecker delta.

If the proportional damping is assumed, then the following relationship holds:

$$C = a_1 L + a_2 M \tag{6}$$

where a_1 and a_2 are some constants. By recalling equations (4) and (5), the orthogonal properties of eigenfunctions with respect to the damping can be shown as follows:

$$\int_D w_r(P)C[w_s(P)]\,\mathrm{d}D(P) = c_r\delta_{rs} = 2\xi_r\omega_r\delta_{rs} \tag{7}$$

where c_r and ξ_r are the rth modal damping coefficient and the rth modal damping ratio, respectively.

2.2. HARMONIC EXCITATION FOR A GENERIC ACTUATION FORCE

By assuming harmonic excitation, the general force function for the generic form of actuation force applied at P_j with magnitude A_j can be expressed by

$$f(P_j, t) = \mathrm{e}^{i\omega t}A_jE(P_j) \tag{8}$$

where $E(P_j)$ is the spatial function of the jth generic actuation force; and ω is the excitation frequency. The response can also be harmonic. From expansion theorem, the displacement response can be assumed to be as follows:

$$w(P, t) = \mathrm{e}^{i\omega t}\sum_{r=1}^{\infty} q_r(\omega)w_r(P) \tag{9}$$

where $q_r(\omega)$ is the frequency-dependent modal amplitude of the rth mode depending on the form of actuation force. By the substitution of equations (8) and (9) into equation (1), equation (1) is then multiplied by $w_s(P)$ and integrated over domain D as follows:

$$q_r(\omega)\Bigg\{\sum_{r=1}^{\infty}\int_D w_s(P)L[w_r(P)]\,\mathrm{d}D(P) + i\omega\sum_{r=1}^{\infty}\int_D w_s(P)C[w_r(P)]\,\mathrm{d}D(P)$$

$$-\omega^2\sum_{r=1}^{\infty}\int_D w_s(P)M(P)w_r(P)\,\mathrm{d}D(P)\Bigg\} = A_j\int_D w_s(P)E(P_j)\,\mathrm{d}D(P). \tag{10}$$

Notice that $\mathrm{e}^{i\omega t}$ term is canceled out. By the substitution of the orthogonal properties of eigenfunctions as shown in equations (4)–(7), equation (10) can be reduced to

$$q_r(\omega)[\omega_r^2 - \omega^2 + i2\xi_r\omega_r\omega] = A_j\int_D w_r(P)E(P_j)\,\mathrm{d}D(P), \quad r = 1, 2, \ldots \tag{11}$$

such that

$$q_r(\omega) = \frac{A_j\displaystyle\int_D w_r(P)E(P_j)\,\mathrm{d}D(P)}{(\omega_r^2 - \omega^2) + i(2\xi_r\omega_r\omega)}, \quad r = 1, 2, \ldots \tag{12}$$

2.3. HARMONIC RESPONSE FOR A GENERIC SENSING DEVICE

In the practical implementation of sensing devices, accelerometers or other sensors can be applied to measure the structural response at location P_i. For harmonic response, the measured quantity S can then be defined by a sensing operator Q operating on the structural displacement response as follows:

$$S(P_i, t) = Q[w(P_i, t)] = e^{i\omega t} Q[w(P_i)]. \tag{13}$$

By the substitution of equation (9) for harmonic response, the measured quantity can be rewritten as follows:

$$S(P_i, t) = e^{i\omega t} \sum_{r=1}^{\infty} q_r(\omega) Q[w_r(P_i)]. \tag{14}$$

By substituting equation (12) into equation (14) and neglecting the harmonic time component, the measured quantity from the sensor at location P_i can be derived as follows:

$$S(P_i) = \sum_{r=1}^{\infty} \frac{A_j \{\int_D w_r(P) E(P_j)\, dD(P)\} \{Q[w_r(P_i)]\}}{(\omega_r^2 - \omega^2) i(2\xi_r \omega_r \omega)}. \tag{15}$$

2.4. FRF BETWEEN THE GENERIC SENSING DEVICE AND THE GENERIC ACTUATION FORCE

The FRF between the response of the ith generic sensing device at location P_i and the magnitude of the jth generic actuation force applied at location P_j can be derived from equation (15) as follows:

$$H_{ij}(\omega) = \frac{S(P_i)}{A_j} = \sum_{r=1}^{\infty} \frac{\{\int_D w_r(P) E(P_j)\, dD(P)\} \{Q[w_r(P_i)]\}}{(\omega_r^2 - \omega^2) + i(2\xi_r \omega_r \omega)}. \tag{16}$$

Now, introduce the symbols as follows:

$$\phi_{r,j}^A = \phi_r^A(P_j) = \int_D w_r(P) E(P_j)\, dD(P) \tag{17}$$

$$\phi_{r,i}^s = \phi_r^s(P_i) = Q[w_r(P_i)] \tag{18}$$

where $\phi_r^A(P)$ and $\phi_r^s(P)$ can be defined as the generic actuator and sensor eigenfunctions respectively. $\phi_{r,j}^A$ and $\phi_{r,j}^s$ can then be identified as the scalar values of the generic actuator and sensor eigenfunctions at locations P_j and P_i, respectively. The FRF can be rewritten as:

$$H_{ij}(\omega) = \frac{S(P_i)}{A_j} = \sum_{r=1}^{\infty} \frac{\phi_{r,j}^A \phi_{r,i}^s}{(\omega_r^2 - \omega^2) + i(2\xi_r \omega_r \omega)}. \tag{19}$$

It is noted that the FRF is expressed in the conventional modal format analogous to the discrete mdof system.

2.5. MEASUREMENT OF FRF

In practical structural modal testing, either roving the actuator with the fixed sensor or roving the sensor with the fixed actuator can be performed. If the generic actuation force is assumed to be fixed and applied at location P_m with magnitude A_m, the generic sensing

device can be applied at N locations all over the structure to measure the system response. A column of the FRF matrix can then be obtained as follows:

$$H_{im}(\omega) = \frac{S(P_i)}{A_m} = \sum_{r=1}^{N} \frac{\phi^A_{r,m}\phi^s_{r,i}}{(\omega_r^2 - \omega^2) + i(2\xi_r\omega_r\omega)}. \tag{20}$$

By observing the above FRF expression, $\phi^A_{r,m} = \phi^A_r(P_m)$, the value of the generic actuator eigenfunction at location P_m, is the fixed scalar value. Therefore, $\phi^s_{r,i} = \phi^s_r(P_i)$, the generic sensor eigenfunction at different location P_i, can be extracted by the curve-fitting process. The rth generic sensor eigenvector (or mode shape), $\{\phi_r\}^s$, containing N components can then be obtained.

If the generic sensing device is assumed to be fixed at location P_m, the generic actuation force is roving to be applied at different locations P_j, $j = 1, 2, \ldots, N$. A row of the FRF matrix can be obtained as follows:

$$H_{mj}(\omega) = \frac{S(P_m)}{A_j} = \sum_{r=1}^{N} \frac{\phi^A_{r,j}\phi^s_{r,m}}{(\omega_r^2 - \omega^2) + i(2\xi_r\omega_r\omega)}. \tag{21}$$

By observing the above FRF expression, $\phi^s_{r,m} = \phi^s_r(P_m)$, i.e. the value of the generic sensor eigenfunction at location P_m, is the fixed scalar value. Therefore, $\phi^A_{r,j} = \phi^A_r(P_j)$, i.e. the value of the generic actuator eigenfunction at different location P_j, can be extracted by curve-fitting algorithms. The rth generic actuator eigenvector, $\{\phi_r\}^A$, can then be obtained. In summary, for practical experimental modal testing roving the sensor with the fixed actuation force will result in the generic sensor eigenvector after the extraction of the modal parameters. In contrast, roving the actuator with the fixed sensor will result in the generic actuator eigenvector.

3. CASE STUDY: ONE-DIMENSIONAL BEAM PROBLEM

In order to demonstrate the validity of the previous general formulation of the FRF, the lateral vibration of a one-dimensional uniform beam problem is considered. The equation of motion for the uniform Euler–Bernoulli beam including damping effect is given in [18], and is neglected here for brevity. Through eigenproblem analysis, an infinite sets of the displacement eigenfunctions $\phi_r(x)$ corresponding to natural frequencies ω_r for various end conditions of beams can be obtained [19]. For harmonic analysis, the displacement response can be assumed from expansion theorem as follows:

$$w(x, t) = e^{i\omega t} \sum_{r=1}^{\infty} q_r(\omega)\phi_r(x) \tag{22}$$

where $q_r(\omega)$ is the rth modal amplitude depending on the form of actuation force.

3.1. HARMONIC EXCITATION FOR DIFFERENT FORMS OF ACTUATORS

3.1.1. *Point force actuators*

Consider the jth harmonic point force applied at x_{f_j} with magnitude F_j as shown in Fig. 1. The general force function can be expressed as follows:

$$f(x_{f_j}, t) = e^{i\omega t} F_j \delta(x - x_{f_j}). \tag{23}$$

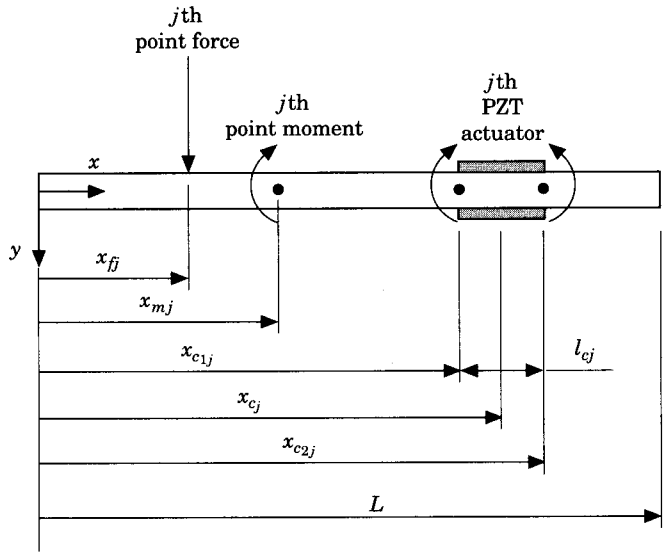

Figure 1. The arrangement and coordinates of three types of actuators in a beam.

In comparison to equation (8), one can easily identify that $A_j = F_j$ and $E(x_{fj}) = \delta(x - x_{fj})$. The point force actuator eigenfunction at location x_{fj}, $\phi^f_{r,j}$, can then be derived based on equation (17) as follows:

$$\phi^f_{r,j} = \phi^f_r(x_{fj}) = \int_0^L \phi_r(x)E(x_{fj})\,\mathrm{d}x = \int_0^L \phi_r(x)\delta(x - x_{fj})\,\mathrm{d}x = \phi_r(x_{fj}). \tag{24}$$

Note that $\phi^f_r(x)$ is the point force actuator eigenfunction, and $\phi^f_{r,j}$ is the point force actuator eigenfunction at location x_{fj}. The point force actuator eigenfunction can be seen actually to be the displacement eigenfunction $\phi_r(x)$.

3.1.2. *Point moment actuators*

For the jth point moment excitation applied as the actuator at location x_{m_j} (Fig. 1), the general force function can be written as:

$$f(x_{m_j}, t) = \mathrm{e}^{i\omega t} M_j \delta'(x - x_{m_j}) \tag{25}$$

where M_j is the magnitude of the point moment, and the derivative of delta function represents the location of the point moment. Therefore, in comparison to equation (8) the magnitude and the spatial function of the point moment can be identified, respectively, as follows:

$$A_j = M_j \tag{26}$$

$$E(x_{m_j}) = \delta'(x - x_{m_j}) \tag{27}$$

The point moment actuator eigenfunction at location x_{m_j}, $\phi^m_{r,j}$, can then be derived from equation (17):

$$\phi^m_{r,j} = \phi^m_r(x_{m_j}) = \int_0^L \phi_r(x)E(x_{m_j})\,\mathrm{d}x = \int_0^L \phi_r(x)\delta'(x - x_{m_j})\,\mathrm{d}x = \phi'_r(x_{m_j}) \tag{28}$$

It is noted that the physical meaning of the point moment actuator eigenfunction $\phi_r^m(x)$ is just the slope eigenfunction of the beam $\phi_r'(x)$.

3.1.3. *PZT actuator*

For pure bending excitation of the PZT actuator, the PZT patches are adhered on the opposite surfaces of the beam and 180° out-of-phase voltage inputs activated. The resulting equivalent actuation forces are two point moments acting on the two edges of the PZT patches as shown in Fig. 1. The general force function can be written as follows [17]:

$$f(x_{c_j}, t) = e^{i\omega t} M_{c_j}[\delta'(x - x_{c_{1j}}) - \delta'(x - x_{c_{2j}})] \tag{29}$$

where

$$x_{c_{1j}} = x_{c_j} - \frac{l_{c_j}}{2} \tag{30}$$

$$x_{c_{2j}} = x_{c_j} + \frac{l_{c_j}}{2} \tag{31}$$

M_{c_j} is the induced equivalent moment by the PZT actuator and is functions of physical properties of the PZT and beam [9–11]. Again, the magnitude and the spatial function of the PZT actuator can be identified as:

$$A_j = M_{c_j} \tag{32}$$

$$E(x_{c_j}) = \delta'(x - x_{c_{1j}}) - \delta'(x - x_{c_{2j}}) \tag{33}$$

Therefore, the PZT actuator eigenfunction at location x_{c_j}, $\phi_{r,j}^c$, can then be determined from equation (17):

$$\phi_{r,j}^c = \phi_r^c(x_{c_j}) = \int_0^L \phi_r(x) E(x_{c_j})\, dx = \int_0^L \phi_r(x)[\delta'(x - x_{c_{1j}}) - \delta'(x - x_{c_{2j}})]\, dx$$

$$= \phi_r'(x_{c_{1j}}) - \phi_r'(x_{c_{2j}}) \tag{34}$$

The physical meaning of the PZT actuator eigenfunction, $\phi_r^c(x)$, can be recognised as the slope difference eigenfunction between the two edges of the PZT patches, $\phi_r'(x_{c1}) - \phi_r'(x_{c2})$. Wang and Wang [15] have shown that for simply supported beams the slope difference eigenfunction is identical to the displacement eigenfunction except multiplying a scaling factor. For cantilever beams, the slope difference eigenfunction is the mirror image of the displacement eigenfunction against the clamped end [17]. Table 1 summarises the characteristics of the three types of actuators.

3.2. HARMONIC RESPONSE MEASURED BY DIFFERENT SENSORS

3.2.1. *Acceleration sensor*

If the ith accelerometer is applied at location x_{a_i} as the sensor (Fig. 2), the measured quantity for harmonic response is:

$$S(x_{a_i}, t) = \ddot{w}(x_{a_i}, t) = -\omega^2 w(x_{a_i})\, e^{i\omega t}. \tag{35}$$

In comparison to equation (13), the sensing operator can be identified as $Q = -\omega^2|_{x = x_{a_i}}$. The accelerometer sensor eigenfunction at location x_{a_i}, $\phi_{r,i}^a$, can be derived from equation (18) as follows:

$$\phi_{r,i}^a = \phi_r^a(x_{a_i}) = Q[\phi_r(x_{a_i})] = -\omega^2 \phi_r(x_{a_i}). \tag{36}$$

TABLE 1

Summary for three types of actuators

Actuator	Magnitude, A_j	Location, x_j	Force function, $f(x_j, t)$	Spatial function, $E(x_j)$	Generic actuator eigenfunction at location x_j, $\phi_{r,j}^A = \int_0^L \phi_r(x)E(x_j)\,dx$	Physical meaning of actuator eigenfunction, $\phi_r^A(x)$
Point force	F_j	x_{f_j}	$F_j\delta(x - x_{f_j})$	$\delta(x - x_{f_j})$	$\phi_{r,j}^f = \phi_r(x_{f_j})$	Displacement, $\phi_r^f(x) = \phi_r(x)$
Point moment	M_j	x_{m_j}	$M_j\delta'(x - x_{m_j})$	$\delta'(x - x_{m_j})$	$\phi_{r,j}^m = \phi_r'(x_{f_j})$	Slope, $\phi_r^m(x) = \phi_r'(x)$
PZT	M_{cj}	$x_{c_{1j}}, x_{c_{2j}}$	$M_{c_j}[\delta'(x - x_{c_{1j}}) - \delta'(x - x_{c_{2j}})]$	$[\delta'(x - x_{c_{1j}}) - \delta'(x - x_{c_{2j}})]$	$\phi_{r,j}^c = \phi_r'(x_{c_{j1}}) - \phi_r'(x_{c_{j2}})$	Slope difference between PZT edges, $\phi_r^c(x) = \phi_r'(x_{c_1}) - \phi_r'(x_{c_2})$

TABLE 2

Summary for three types of sensors

Sensor	Location, x_i	Measured quantity, $S(x_i) = Q[w(x_i)]$	Sensing operator, Q	Generic sensor eigenfunction at location x_i, $\phi_{r,i}^s = Q[\phi_r(x_i)]$	Physical meaning of sensor eigenfunction, $\phi_r^s(x)$
Accelerometer	x_{a_i}	$-\omega^2 w(x_{a_i})$	$-\omega^2\|_{x = x_{a_i}}$	$\phi_{r,i}^a = -\omega^2\phi_r(x_{a_i})$	Displacement, $\phi_r^a(x) = -\omega^2\phi_r(x)$
Rotational sensor	x_{θ_i}	$\left.\dfrac{\partial w(x)}{\partial x}\right\|_{x = x_{\theta_i}}$	$\left.\dfrac{\partial}{\partial x}\right\|_{x = x_{\theta_i}}$	$\phi_{r,i}^\theta = \phi_r'(x_{\theta_i})$	Slope, $\phi_r^\theta(x) = \phi_r'(x)$
PVDF sensor	$x_{p_{i1}}, x_{p_{i2}}$	$K_p\left[\left.\dfrac{\partial w(x)}{\partial x}\right\|_{x = x_{p1i}} - \left.\dfrac{\partial w(x)}{\partial x}\right\|_{x = x_{p2i}}\right]$	$K_p\left[\left.\dfrac{\partial}{\partial x}\right\|_{x = x_{p1i}} - \left.\dfrac{\partial}{\partial x}\right\|_{x = x_{p2i}}\right]$	$\phi_{r,i}^p = K_p[\phi_r'(x_{p_{1i}}) - \phi_r'(x_{p_{2i}})]$	Slope difference between PVDF edges, $\phi_r^p(x) = K_p[\phi_r'(x_{p_1}) - \phi_r'(x_{p_2})]$

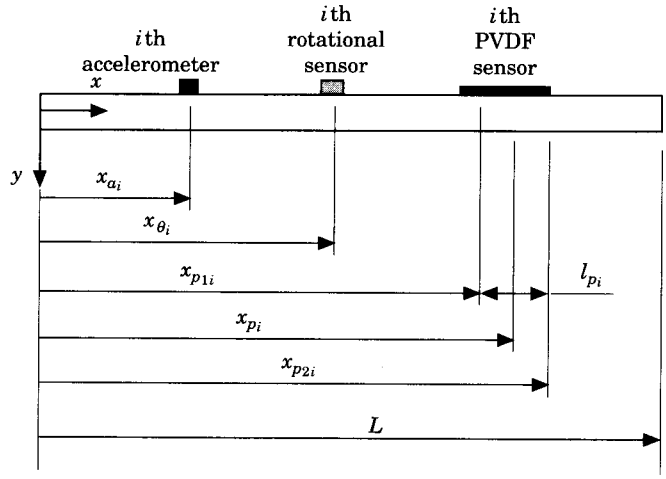

Figure 2. The arrangement and coordinates of three types of sensors in a beam.

It is noted that the accelerometer sensor eigenfunction $\phi_r^a(x)$ is simply the displacement eigenfunction $\phi_r(x)$ multiplying the scaling factor $-\omega^2$.

3.2.2. *Rotational sensor*

For the ith rotational sensor applied at location x_{θ_i}, as shown in Fig. 2, the slope of the beam can be detected. The measured quantity neglecting the harmonic time component can be shown as follows:

$$S(x_{\theta_i}) = \left.\frac{\partial w(x)}{\partial x}\right|_{x = x_{\theta_i}}. \tag{37}$$

By comparison to equation (13), the sensing operator can then be identified as:

$$Q = \left.\frac{\partial}{\partial x}\right|_{x = x_{\theta_i}} \tag{38}$$

and the rotational sensor eigenfunction at location x_{θ_i}, $\phi_{r,i}^{\theta}$ can be derived from equation (18) as follows:

$$\phi_{r,i}^{\theta} = \phi_r^{\theta}(x_{\theta_i}) = Q[\phi_r(x_{\theta_i})] = \phi_r'(x_{\theta_i}). \tag{39}$$

Note that the rotational sensor eigenfunction $\phi_r^{\theta}(x)$, similar to the point moment actuator eigenfunction $\phi_r^m(x)$, is just the slope eigenfunction of the beam $\phi_r'(x)$.

3.2.3. *PVDF sensor*

When a strip of PVDF patch is applied as the sensing device (Fig. 2), the measured voltage output from the ith PVDF patch with length l_{p_i} can be shown to be as follows [17]:

$$S(x_{p_i}) = K_p \sum_{r=1}^{\infty} q_r(\omega)[\phi_r'(x_{p_{1i}}) - \phi_r'(x_{p_{2i}})] \tag{40}$$

where

$$x_{p_{1i}} = x_{p_i} - \frac{l_{p_i}}{2} \tag{41}$$

$$x_{p_{2i}} = x_{p_i} + \frac{l_{p_i}}{2} \tag{42}$$

and K_p is some constant related to the PVDF and beam material properties and physical dimensions. In comparison to equation (14), one can identify the sensing operator as:

$$Q = K_p\left[\frac{\partial}{\partial x}\bigg|_{x = x_{p_{1i}}} - \frac{\partial}{\partial x}\bigg|_{x = x_{p_{2i}}}\right] \tag{43}$$

The PVDF sensor eigenfunction at location x_{p_i}, $\phi^p_{r,i}$, can then be determined from equation (18):

$$\phi^p_{r,i} = \phi^p_r(x_{p_i}) = Q[\phi_r(x_{p_i})] = K_p[\phi'_r(x_{p_{1i}}) - \phi'_r(x_{p_{2i}})] \tag{44}$$

It is noted that the PVDF sensor eigenfunction $\phi^p_r(x)$, similar to the PZT actuator eigenfunction $\phi^c_r(x)$, is still the slope difference eigenfunction between the two edges of the PVDF patch, $\phi'_r(x_{p1}) - \phi'_r(x_{p2})$. Table 2 summarises the characteristics of the three types of sensors.

3.3. MEASUREMENT OF THE FRF

Three types of actuators and three types of sensors are illustrated and characterised. The actuator and sensor eigenfunctions at a location are properly identified and physically interpreted as shown in Tables 1 and 2. Any combination of actuator and sensor can be selected to perform structural modal testing. For conventional structural modal testing, the point force is generally applied as the actuator, while the accelerometer is chosen as the sensor. From equation (19), the FRF between the ith accelerometer at location x_{a_i} and the jth point force with magnitude F_j at location x_{f_j} can be determined as follows:

$$H_{ij}(\omega) = \frac{\ddot{w}(x_{a_i})}{F_j} = \sum_{r=1}^{N} \frac{\phi^f_{r,j}\phi^a_{r,i}}{(\omega_r^2 - \omega^2) + i(2\xi_r\omega_r\omega)} = -\omega^2 \sum_{r=1}^{N} \frac{\phi_{r,j}\phi_{r,i}}{(\omega_r^2 - \omega^2) + i(2\xi_r\omega_r\omega)} \tag{45}$$

where $\phi_{r,j} = \phi_r(x_{f_j})$ and $\phi_{r,i} = \phi_r(x_{a_i})$. It is noted that from Tables 1 and 2 both the point force actuator eigenfunction at location x_{f_j}, $\phi^f_{r,j}$, and the accelerometer sensor eigenfunction at location x_{a_i}, $\phi^a_{r,i}$, are known to be the values of the displacement eigenfunction at the corresponding locations. Therefore, the experimental modal testing procedure can be performed by either roving the point force actuator with the fixed accelerometer or roving the accelerometer with the fixed point force actuator. The displacement eigenvector (or mode shape) $\{\phi_r\}$ can be always extracted by curve-fitting algorithms from a column or a row of FRF matrix that is experimentally determined.

For another example, let the PZT actuator and the accelerometer sensor be selected for structural modal testing. The resulting FRF between the ith accelerometer at location x_{a_i} and the jth PZT actuator with the equivalent moment magnitude M_{c_j} at location x_{c_j} can be derived from equation (19) as follows:

$$H_{ij}(\omega) = \frac{\ddot{w}(x_{a_i})}{M_{c_j}} = \sum_{r=1}^{N} \frac{\phi^c_{r,j}\phi^a_{r,i}}{(\omega_r^2 - \omega^2) + i(2\xi_r\omega_r\omega)} = -\omega^2 \sum_{r=1}^{N} \frac{[\phi'_r(x_{c_{1j}}) - \phi'_r(x_{c_{2j}})][\phi_{r,i}]}{(\omega_r^2 - \omega^2) + i(2\xi_r\omega_r\omega)} \tag{46}$$

TABLE 3

Physical meanings of extracted mode shapes for different combinations of actuators and sensors with respect to test procedures

Sensor	Actuator	Physical meaning of the extracted mode shape for roving actuator with fixed sensor (a row of FRF matrix is obtained)	Physical meaning of the extracted mode shape for roving sensor with fixed actuator (a column of FRF matrix is obtained)
Accelerometer	Point force	Displacement mode shape	Displacement mode shape
Accelerometer	Point moment	Slope mode shape	Displacement mode shape
Accelerometer	PZT	Slope difference mode shape	Displacement mode shape
Rotational	Point force	Displacement mode shape	Slope mode shape
Rotational	Point moment	Slope mode shape	Slope mode shape
Rotational	PZT	Slope difference mode shape	Slope mode shape
PVDF	Point force	Displacement mode shape	Slope difference mode shape
PVDF	Point moment	Slope mode shape	Slope difference mode shape
PVDF	PZT	Slope difference mode shape	Slope difference mode shape

From the observation of the above FRF expression, conclusions can be made as follows.

(1) When roving the accelerometer with the fixed PZT actuator, a row of the FRF matrix can be determined. One can then obtain the accelerometer sensor mode shapes, i.e. the displacement mode shapes, after the extraction of modal parameters from the FRFs.
(2) When roving the PZT actuator with the fixed accelerometer, a column of the FRF matrix can be determined. One can obtain the PZT actuator mode shapes, i.e. the slope difference mode shapes between the two edges of the PZT patch, after the extraction of modal parameters from the FRFs.

Nine combinations of the three types of actuators and sensors can be selected to perform the structural modal testing. Similar derivations of FRFs can be determined. The testing procedure either roving the actuator with the fixed sensor or roving the sensor with the fixed actuator will result in different physical meanings for the extracted mode shapes as summarised in Table 3. In summary, the testing procedure will determine the extracted mode shapes being actuator or sensor mode shapes. The physical meanings of the extracted mode shapes will be interpreted by the forms of actuators and sensors. The experimental modal testing of the cantilever beam for four combinations of actuators and sensors, such as point force/accelerometer, PZT actuator/accelerometer, point force/PVDF sensor and PZT actuator/PVDF sensor, are theoretically [17] and experimentally [20] demonstrated. The theoretical formulation of this work is thus verified. Further study in experimental verification for plate structures subject to various forms of actuators and sensors is also under investigation.

4. CONCLUSIONS

This work generalises the formulation of FRFs continuous structure systems subject to various forms of actuators and sensors. The generic actuator eigenfunction and generic sensor eigenfunction are defined and physically interpreted, respectively. This work provides the theoretical base for the applications of various forms of actuators and sensors to structural modal testing. Conventional curve-fitting algorithms are suitable for extracting the modal parameters, including natural frequencies, modal damping ratios and mode shapes. The testing procedure either roving the sensor with the fixed actuator or roving the actuator with the fixed sensor will result in sensor eigenfunction or actuator eigenfunction after the extraction of modal parameters, respectively. The forms of actuators and sensor will then characterise the physical meanings of the extracted mode shapes. The lateral vibration of a one-dimensional beam problem considering three types of actuators and three types of sensors is illustrated to demonstrate the generic formulation of FRF. In particular, the applications of smart materials, such as PZT actuators and PVDF sensors, to smart structural testing is demonstrated. The theoretical formulation in this work is also applicable to other continuous structure systems as well as other available types of actuators and sensors.

ACKNOWLEDGEMENT

This work was partially supported by National Science Council, Republic of China, under contract number NSC87-2212-E-020-003.

REFERENCES

1. D. J. EWINS 1986 *Modal Testing: Theory and Practice*. Letchworth, U.K.: Research Studies Press.
2. H. H. CUDNEY and D. J. INMAN 1989 *The International Journal of Analytical and Experimental Modal Analysis* **4**, 138–143. Determining damping mechanisms in a composite beam by experimental modal analysis.
3. K. M. M. EL-DEEB and R. ROYLES 1992 *The International Journal of Analytical and Experimental Modal Analysis* **7**, 51–63. Modal examination of an echinodome.
4. S. HAN and K. G. MCCONNELL 1991 *The International Journal of Analytical and Experimental Modal Analysis* **6**, 147–159. Analysis of frequency response functions affected by the coupled modes of the structure.
5. D. L. BROWN, R. J. ALLEMANG, R. ZIMMERMAN and M. MERGEAY 1979 *SAE Paper*, 790221. Parameter estimation techniques for modal analysis.
6. P. SRIRAM, J. I. CRAIG and S. HANAGUD 1995 *The International Journal of Analytical and Experimental Modal Analysis*. A scanning laser doppler vibrometer for modal testing.
7. F. P. SUN, L. D. MITCHELL and J. R. F. ARRUDA 1993 *Experimental Techniques* **17**(3), 31–37. Mode decoupling considerations in mode shape measurements of a plate with monoexcitation and laser doppler vibrometer.
8. KISTLER INSTRUMENT CORPORATION 1994 *Product Catalog*. Amherst, New York.
9. E. F. CRAWLEY and J. DE LUIS 1987 *AIAA Journal* **25**, 1373–1385. Use of piezoelectric actuators as elements of intelligent structures.
10. B. T. WANG and C. A. ROGERS 1991 *Journal of Intelligent Material Systems and Structures* **2**, 38–58. Modeling of finite-length spatially distributed induced strain actuators for laminate beams structures.
11. E. K. DIMITRIADIS, C. R. FULLER and C. A. ROGERS 1991 *Journal of Vibration and Acoustics* **113**, 100–107. Piezoelectric actuators for distributed vibration excitation of thin plate.
12. J. E. HUBBARD 1987 *Noise-Con* **87**, 407–412. Distributed sensors and actuators for vibration control in elastic components.
13. C. K. LEE and F. C. MOON 1990 *Journal of Applied Mechanics* **57**, 434–441. Modal Sensors/Actuators.
14. F. P. SUN, C. LIANG and C. A. ROGERS 1994 *Proceedings of the 1994 SEM Spring Conference and Exhibits*, 871–879. Experimental modal testing using piezoceramic patches as collocated sensor-actuators.
15. B. T. WANG 1996 *Journal of Intelligent Material Structures and Systems* **7**, 390–398. Characterization of transfer functions for piezoceramic and conventional transducers.
16. C. NORWOOD 1995 *Proceedings of INTER-NOISE 95*, 1337–1340. The measurement of natural frequencies and mode shapes of submerged cylinder using PVDF strip excitation.
17. B. T. WANG and C. C. WANG 1997 *Journal of Smart Materials and Structures* **6**, 106–116. Feasibility analysis of using piezoceramic transducers for cantilever beam modal testing.
18. L. MEIROVITCH 1967 *Analytical Methods in Vibrations*. New York: MacMillan Company.
19. S. S. RAO 1990 *Mechanical Vibrations*. Reading, MA. Addison-Wesley Publishing.
20. B. T. WANG and C. C. WANG 1997 *Journal of Technology* **12**, 419–425. Applications of piezoceramic actuators to experimental modal testing of cantilever beam.